

Supporting Information

Effect of chemical substitution on the construction of boroxine-based supramolecular crystalline polymers featuring B←N dative bonds

Subhrajyoti Bhandary,^a Rahul Shukla,^b and Kristof Van Hecke*^a

^a XStruct, Department of chemistry, Krijgslaan 281-S3, Ghent University, Belgium

^b Department of Chemistry, Ben-Gurion University of the Negev, Beer Sheva, 841051, Israel.

E-mail: kristof.vanhecke@ugent.be

Table of Contents

S1. Materials, mechanochemical synthesis and single-crystal growth

S2. X-ray diffraction measurements and single-crystal structure determination

S3. Computational details

S4. CSD search

S5. References

S1. Materials, mechanochemical synthesis, and single-crystal growth

Differently substituted (*para*-H/-OCH₃/-F/-Cl/-Br) phenylboronic acids and the 4-diazabicyclo[2.2.2]octane (DABCO) ligand were purchased from Aldrich. Three stoichiometric equivalents of each phenylboronic acid and one equivalent of DABCO were taken and placed in a ceramic motor at ambient condition (15–18 °C). The facile desolvation of water from phenylboronic acids to form the corresponding phenylboroxines is a well-known process (ref no. 10f in the main manuscript). The mixture was gently ground by a pestle for 40–45 minutes without any solvent dropping. The ground material of five phenylboroxine-DABCO adducts (*p*-H, *p*-OMe, *p*-F, *p*-Cl, and *p*-Br) were crystallized further at various conditions (Table S1) to obtain suitable single crystals for single-crystal X-ray diffraction analysis.

Table S1. Single-crystal growth conditions for all five phenylboroxine-DABCO adducts (*p*-H, *p*-OCH₃, *p*-F, *p*-Cl, and *p*-Br)

Adduct	Crystallization solvent	Crystallization temperature
<i>p</i> -H	toluene	70 °C (oven)
	DCM	15-18 °C (RT)
<i>p</i> -OMe	toluene	70 °C (oven)
<i>p</i> -F	toluene	70 °C (oven)
	DCM	15-18 °C (RT)
<i>p</i> -Cl	toluene	70 °C (oven)
<i>p</i> -Br	toluene	70 °C (oven)

S2. X-ray diffraction measurements and single-crystal structure determination

Powder X-ray diffraction measurements for all crystalline (bulk) adducts were measured on a Bruker D8 Advance diffractometer with Cu K α radiation. Diffractograms were collected at room temperature from 5° to 55° (2 θ).

For all adduct structures, single crystal X-ray diffraction (SCXRD) data were collected on a Rigaku Oxford Diffraction SuperNova dual source (Cu at zero) diffractometer equipped with an Atlas CCD detector using ω scans and monochromated Cu K α radiation ($\lambda = 1.54184 \text{ \AA}$), at room temperature. Data reduction was performed with the *CrysAlisPro* software package.^[1] The crystal structures were solved by Intrinsic Phasing using the *ShelXT* program.^[2] All structures were refined by full-matrix least-squares on F² using the *ShelXL* 2018/3 program package,^[3] by means of the *Olex2* interface.^[4] All non-hydrogen atoms were refined anisotropically. All hydrogen atoms were positioned geometrically and refined using a riding model.

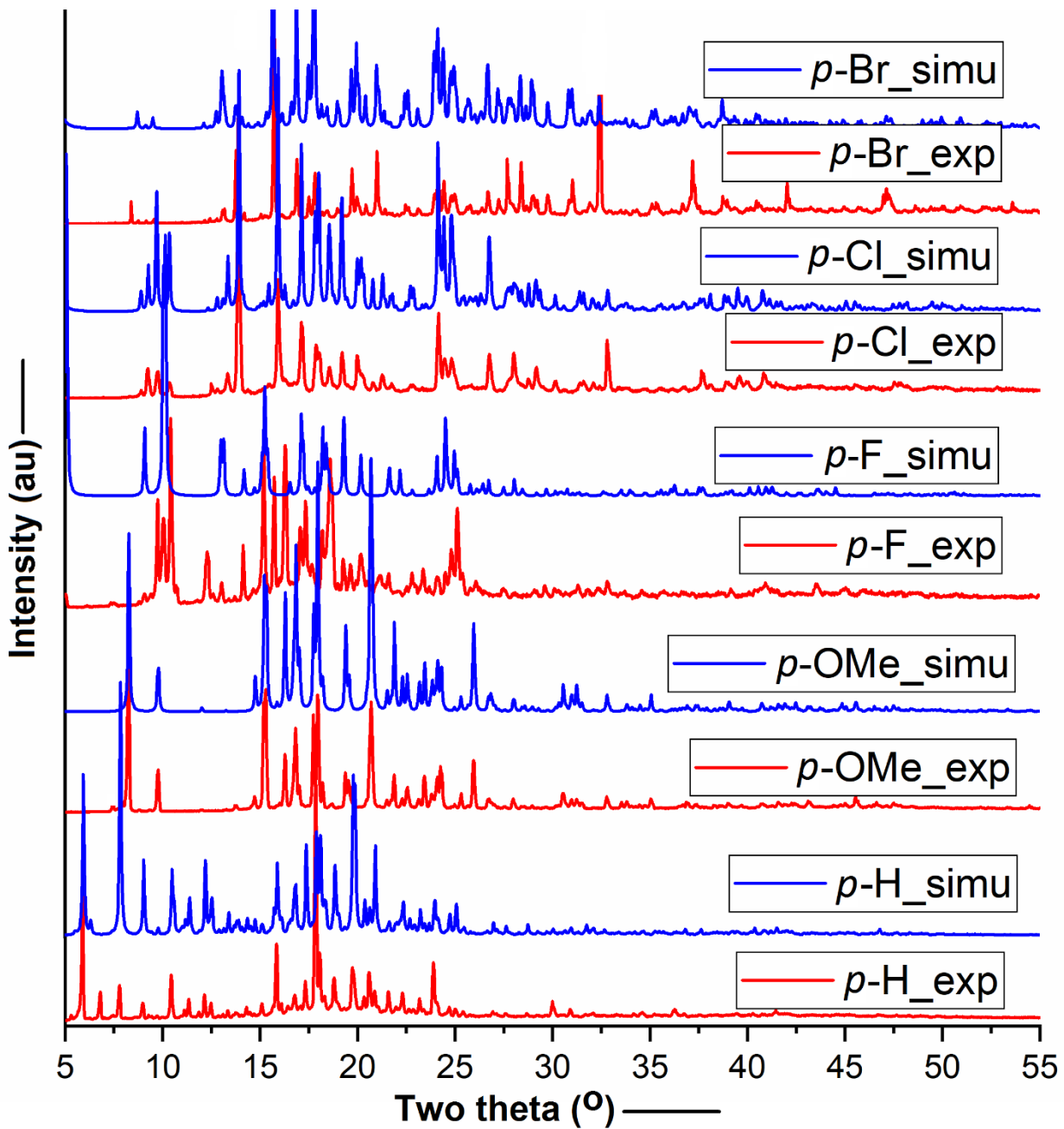


Figure S1. Overlay of experimental PXRD patterns of all five synthesized (bulk) adducts showing sharp diffraction patterns and highly crystalline materials (red), and the simulated PXRD patterns, based on the five crystal structures (blue). Small differences between experimental and simulated PXRD patterns can be due to preferred crystallite (plate and needle-like morphology) orientation, and solvent mask used (for *p*-F) during refinement, to account for diffuse solvent contribution in solvent accessible voids.

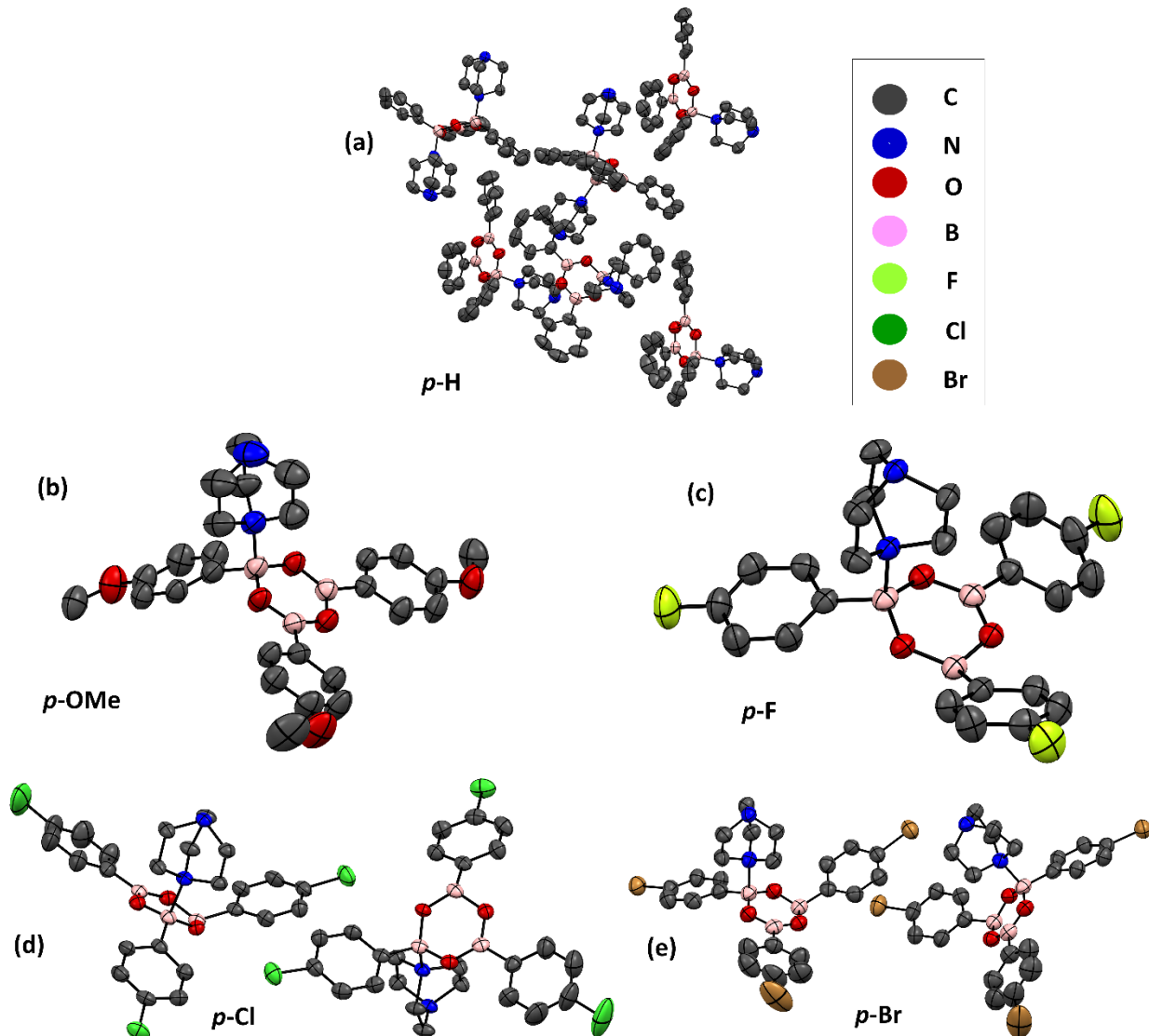


Figure S2. Thermal ellipsoidal plots (drawn at the 50% probability level) of the asymmetric units for all five crystalline adducts: (a-b) molecular crystals (*p*-H and *p*-OMe) and (c-e) polymeric crystals (*p*-Cl, *p*-Cl, and *p*-Br). All hydrogen atoms and additional guest toluene molecules for *p*-Cl and *p*-Br have been omitted for clarity.

Table S2. Crystal data and structure refinement parameters for the five crystalline adducts

Identification code	<i>p</i> -H	<i>p</i> -OMe	<i>p</i> -F	<i>p</i> -Cl	<i>p</i> -Br
CCDC	2131638	2131639	2131640	2131641	2131642
Empirical formula	C ₇₈ H ₉₃ B ₉ N ₈ O ₉	C ₂₇ H ₃₃ B ₃ N ₂ O ₆	C ₂₄ H ₂₄ B ₃ F ₃ N ₂ O ₃	C ₅₅ H ₅₆ B ₆ Cl ₆ N ₄ O ₆	C ₅₅ H ₅₆ B ₆ Br ₆ N ₄ O ₆
Formula weight	1383.89	513.98	477.88	1146.59	1413.35
Temperature/K	290(2)	290(2)	290(2)	290(2)	290(2)
Crystal system	monoclinic	monoclinic	monoclinic	triclinic	triclinic
Space group	<i>P</i> 2 ₁ / <i>c</i>	<i>P</i> 2 ₁ / <i>n</i>	<i>C</i> 2/ <i>c</i>	<i>P</i> -1	<i>P</i> -1
a/Å	16.2604(2)	11.81600(10)	34.9799(7)	7.4070(2)	7.40892(14)
b/Å	32.0503(3)	12.7112(2)	7.38830(10)	19.9475(6)	20.3510(5)
c/Å	30.5203(3)	18.3186(2)	19.5336(4)	20.9507(7)	21.2329(8)
α/°	90	90	90	66.186(3)	66.065(3)
β/°	103.2310(10)	100.2500(10)	94.675(2)	84.935(2)	85.056(2)
γ/°	90	90	90	89.714(2)	89.7360(17)
Volume/Å ³	15483.5(3)	2707.46(6)	5031.51(16)	2819.29(16)	2913.66(15)
Z	8	4	8	2	2
ρ _{calc} /gcm ⁻³	1.187	1.261	1.262	1.351	1.611
μ/mm ⁻¹	0.598	0.701	0.803	3.206	5.392
F(000)	5872.0	1088.0	1984.0	1188.0	1404.0
Crystal size/mm ³	0.2 × 0.13 × 0.04	0.18 × 0.14 × 0.05	0.22 × 0.14 × 0.05	0.16 × 0.1 × 0.04	0.18 × 0.12 × 0.04
Radiation	Cu Kα (λ = 1.54184)	Cu Kα (λ = 1.54184)	Cu Kα (λ = 1.54184)	Cu Kα (λ = 1.54184)	Cu Kα (λ = 1.54184)
2θ range for data collection/°	5.584 to 147.752	8.284 to 147.812	5.07 to 147.458	5.172 to 147.834	7.826 to 147.638
Index ranges	-20 ≤ h ≤ 20, -39 ≤ k ≤ 30, -37 ≤ l ≤ 37	-14 ≤ h ≤ 14, -15 ≤ k ≤ 15, -22 ≤ l ≤ 22	-43 ≤ h ≤ 42, -9 ≤ k ≤ 8, -24 ≤ l ≤ 24	-9 ≤ h ≤ 9, -24 ≤ k ≤ 24, -26 ≤ l ≤ 26	-9 ≤ h ≤ 9, -25 ≤ k ≤ 25, -26 ≤ l ≤ 26
Reflections collected	147597	26173	22728	51594	19520
Independent reflections	30886 [R _{int} = 0.0672, R _{sigma} = 0.0547]	5430 [R _{int} = 0.0272, R _{sigma} = 0.0185]	5026 [R _{int} = 0.0421, R _{sigma} = 0.0295]	11242 [R _{int} = 0.0582, R _{sigma} = 0.0441]	19520 [R _{int} = ?, R _{sigma} = 0.0180]
Data/restraints/parameters	30886/468/1947	5430/315/396	5026/0/316	11242/180/733	19520/270/734
Goodness-of-fit on F ²	0.984	1.034	1.025	1.027	1.056
Final R indexes [I > 2σ (I)]	R ₁ = 0.0562, wR ₂ = 0.1340	R ₁ = 0.0534, wR ₂ = 0.1477	R ₁ = 0.0495, wR ₂ = 0.1391	R ₁ = 0.0632, wR ₂ = 0.1689	R ₁ = 0.0818, wR ₂ = 0.2383
Final R indexes [all data]	R ₁ = 0.1287, wR ₂ = 0.1820	R ₁ = 0.0716, wR ₂ = 0.1672	R ₁ = 0.0664, wR ₂ = 0.1553	R ₁ = 0.0904, wR ₂ = 0.1935	R ₁ = 0.0918, wR ₂ = 0.2492
Largest diff. peak/hole / e Å ⁻³	0.18/-0.17	0.29/-0.18	0.20/-0.19	0.94/-0.47	1.26/-0.42
Flack parameter	NA	NA	NA	NA	NA

S3. Computational details

All quantum mechanical calculations were performed at the B3LYP-D3/6-311+g (d,p) level using *Gaussian 16*.^[5] The topological analysis of electron density (QTAIM) was performed using the AIMALL suite (version 19.10.12)^[6] and selected topological parameters, *i.e.* electron density (ρ), Laplacian ($\nabla^2\rho$), local potential energy (V_b)/dissociation energy (DE), at the B-N bond critical points, and electron delocalization index (DI) were calculated.

S4. CSD search: polymeric metal-free crystal structures containing B-N bonds

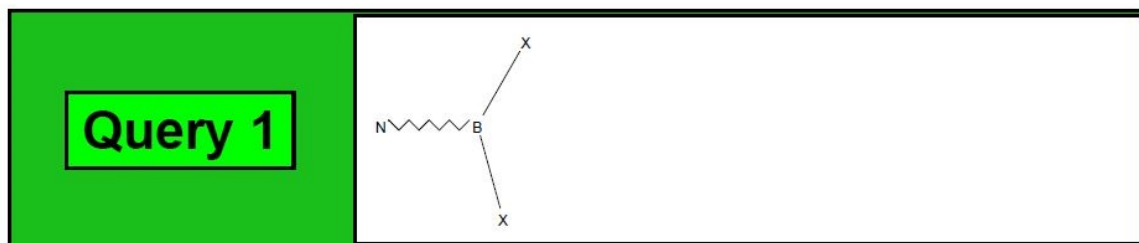
Search Overview

Search:	search3	
Date/Time done:	Wed Dec 22 21:45:42 2021	
Database(s):	CSD version 5.42 updates (Feb 2021) CSD version 5.42 (November 2020)	
Restriction Info:	No refcode restrictions applied	
Filters:	3D coordinates determined No ions Only Organics	No errors Only Single crystal structures
Percentage Completed:	100%	
Number of Hits:	31	

Single query used. Search found structures that:

match

Query 1



S5. References

- [1] Rigaku Oxford Diffraction, (2020), CrysAlisPro Software system, Rigaku Corporation, Oxford, UK.
- [2] G. M. Sheldrick, *Acta Crystallogr. Sect. A*, 2015, **71**, 3-8.
- [3] G. M. Sheldrick, *Acta Crystallogr. Sect. C*, 2015, **71**, 3-8.
- [4] O. V. Dolomanov , L. J. Bourhis , R. J. Gildea , J. A. K. Howard and H. Puschmann, *J. Appl. Crystallogr.*, 2009, **42**, 339-341.
- [5] M. J. Frisch, G. W. Trucks, H. B. Schlegel, G. E. Scuseria, M. A. Robb, J. R. Cheeseman, G. Scalmani, V. Barone, G. A. Petersson, H. Nakatsuji, X. Li, M. Caricato, A. V. Marenich, J. Bloino, B. G. Janesko, R. Gomperts, B. Mennucci, H. P. Hratchian, J. V. Ortiz, A. F. Izmaylov, J. L. Sonnenberg, D. Williams-Young, F. Ding, F. Lipparini, F. Egidi, J. Goings, B. Peng, A. Petrone, T. Henderson, D. Ranasinghe, V. G. Zakrzewski, J. Gao, N. Rega, G. Zheng, W. Liang, M. Hada, M. Ehara, K. Toyota, R. Fukuda, J. Hasegawa, M. Ishida, T. Nakajima, Y. Honda, O. Kitao, H. Nakai, T. Vreven, K. Throssell, J. A. Montgomery, Jr., J. E. Peralta, F. Ogliaro, M. J. Bearpark, J. J. Heyd, E. N. Brothers, K. N. Kudin, V. N. Staroverov, T. A. Keith, R. Kobayashi, J. Normand, K. Raghavachari, A. P. Rendell, J. C. Burant, S. S. Iyengar, J. Tomasi, M. Cossi, J. M. Millam, M. Klene, C. Adamo, R. Cammi, J. W. Ochterski, R. L. Martin, K. Morokuma, O. Farkas, J. B. Foresman, D. J. Fox, *Gaussian 16*, Revision C.01, Gaussian, Inc., Wallingford CT, 2016.
- [6] T. A. Keith, *AIMALL*, version 19.10.12; TK Gristmill Software, Overland Park KS, USA, 2019, aim.tkgristmill.com